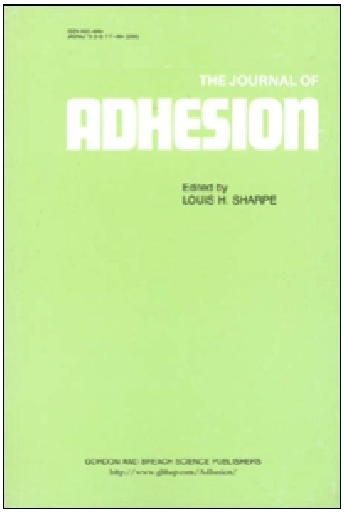

The Journal of Adhesion
Publication details, including instructions for authors and subscription information:
http://www.informaworld.com/smpp/title~content=t713453635

Comparison Between Experimental and Theoretical Analysis of Stress Distribution in Adhesively-Bonded Joints: Tenon and Mortise Joints and Single-Lap Joints

Bernard Fargette[a]; Yvon Gilibert[a]; Lucien Rimlinger[a]
[a] Université de Reims Champagne Ardenne, Reims, Cedex, France

To cite this Article Fargette, Bernard , Gilibert, Yvon and Rimlinger, Lucien(1996) 'Comparison Between Experimental and Theoretical Analysis of Stress Distribution in Adhesively-Bonded Joints: Tenon and Mortise Joints and Single-Lap Joints', The Journal of Adhesion, 59: 1, 159 — 170

To link to this Article: DOI: 10.1080/00218469608011085

URL: http://dx.doi.org/10.1080/00218469608011085

J. Adhesion, 1996, Vol. 59, pp. 159–170
Reprints available directly from the publisher
Photocopying permitted by license only

Comparison Between Experimental and Theoretical Analysis of Stress Distribution in Adhesively-Bonded Joints: Tenon and Mortise Joints and Single-Lap Joints*

BERNARD FARGETTE, YVON GILIBERT** and LUCIEN RIMLINGER

Université de Reims Champagne Ardenne, ER-CM2S, Laboratoire de Science des Matériaux, BP 1039, 51687 Reims Cedex, France

(In final form January 20, 1996)

We have studied the agreement between theoretical computations and experimental results of surface strains of bonded joints of two types: tenon and mortise, and single-lap joints, for different lengths of the lap. For instance, with the single-lap joint, we have tested four lengths of the overlap from 14 mm to 88 mm. Surface strains are measured by an extensometrical method with electrical gauges, when the specimen is loaded in uniaxial traction on a universal testing machine.

Experimental results and computations made by an improved method, such as the asymptotic expansions method, agree but only if the global traction load applied on the specimen is low, or if the overlap in respect with the others dimensions of the section of test specimen is long.

In these joints, effectively, stress fields are disrupted near the butts and become very difficult to compute. Actually, near the ends of the overlap, stresses can reach high limits with only low global load applied on the test specimen. With a short length of the overlap, linear behaviour disappears almost totally because of a strong interaction of the two perturbed fields. On the contrary, with a high length of overlap, stress fields become linear on the major part of the overlap, even with a high tensile load applied on the specimen. So, the length of the overlap has a great effect on the linear behaviour of the joint.

KEY WORDS: Surface strains in adhesive joints; stress fields; effect of lap length; asymptotic expansions method; analytical computation; comparison of theory and experiment.

1. INTRODUCTION

Bonded assemblies has become more and more used in technical fields such as mechanical design or building. Knowledge of mechanical strength of these assemblages is of great practical importance. Nevertheless, computation of bonded joints which must withstand a given load has not yet become a common practice in a design office. Design of bonded joints is generally the result of use of empirical rules,

*Presented at the International Adhesion Symposium, *IAS'94 Japan*, at the 30th Anniversary Meeting of the Adhesion Society of Japan, Yokohama, Japan, November 6–10, 1994.

**Corresponding author.

which give the shapes of joints where the adhesive is subjected mainly to shear stress and avoid normal traction stress or "peel stress" which weakens the joint. Mechanical stresses in joints are complex, even for a simple shape of joint or simple load such as a uniaxial tensile load. So computation in real technical applied cases, with combined stresses, are not easy. Besides, in a traction test of a specimen, early damage in the adhesive can occur far short of the ultimate strength of a joint. Experimentally, precise mechanical behaviour of the adhesive in a bonded joint which would show the start of cracking is difficult to carry measure, and electrical strain gauges glued on the external surface of adherends, or acoustic emission, have nowadays become two useful methods to study the damage in bonded joints.

The symmetry of the double lap bonded joint nearly eliminates the flexure in the outer adherends. Also, many experimental studies have been directed toward a better knowledge of the precise mechanical behaviour of this type of joint[1-12].

This symmetry is again present in the tenon and mortise joint. Besides, adhesive can be put at the slot ends of the lap to form front layers, but they are generally fragile, because they work in normal stresses, while the two laps work principally in shear stress. Nevertheless, the tenon and mortise joint is very rarely studied[13,14] because of the difficulty of modeling the angular singularity at each corner in analytical studies, and the difficulties of machining the mortise in experimental studies or technical applications[15].

The single-lap joint, studied in early analysis[16], is non-symmetrical and important flexures appear in a test under traction load. The half-thickness type joint derives from this single-lap joint[17,18] and allows a decrease in the misalignement of the load. However, this does not eliminate totally the flexure of adherends[19-21]. Moreover, like the tenon and mortise joint, adhesive can fill the end slots, to strengthen this joint, but this possibility has not been studied extensively[13].

2. EXPERIMENTAL ANALYSIS

2.1. Specimen Preparation

The geometrical shape of specimens is given in Figure 1. Adherends are made of mild steel containing 0.18% Carbon (French Standard XC 18 equivalent to SAE-AISI 1017) with a ferritic microstructure, or of "FORTAL HR" (trade mark of Aluminium Pechiney), a structural hardening aluminium alloy. Bars, with a square cross section 10×10 mm, are obtained by milling and finishing on a horizontal surface grinding machine. A thread, ISO 12×150, is machined at an end of the bar in order to screw the specimen into special knee joints, to fit in the jaws of a univeral testing machine. Steps and tenon are easily made by conventional machining, but the mortise requires wire spark machining. The finish of substrates is obtained by sandblasting with an alumina sand, AVB 150 (trade mark of Vapor Blast), with a particle diameter selected so as to give a total depth roughness, Rt, close to the average size of the adhesive fillers[5,9,10,11,22].

We used the commercial adhesive "EPONAL 317" (French registered trade mark of CECA) which is a two component system: an epoxy resin containing mineral

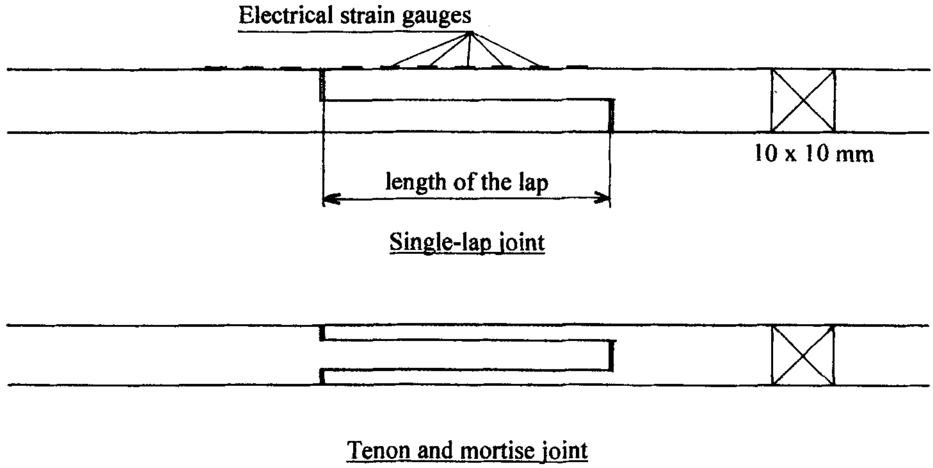

FIGURE 1 Geometrical shapes of studied specimens: half thickness single-lap joints, and tenon and mortise joints. Thickness of adhesive layers; $e_j = 0.4$ mm, Thickness of adherends; single lap-$e_T = 4.8$ mm, tenon-$e_t = 4.6$ mm, Mortise-$e_m = 2.3$ mm.

fillers and a hardening agent. An overlayer of adhesive is put on each surface in order to drive away the bubbles when the two surfaces come together during bonding. To line up the bars, the two pieces are put on a vee block[23] for this operation. A strip of PTFE is put on the butt surfaces to avoid bonding in these places. Polymerisation begins 20 minutes after mixing, and hardening needs a few hours at room temperature (20°C). After hardening, the adhesive shows an elastic, brittle behaviour.

The electrical strain gauges are placed at different points (generally with a 2 mm step) on the external surfaces of metallic adherends, in order to verify the agreement between the experimental and analytical results of surface strains. In fact, as the gauge length is 1.5 mm, the strain measured using these gauges, is the mean strain along a gauge length. This must be kept in mind for experimental values near the end of lap, because there exists there a steep strain gradient. Nevertheless, the gauges located in the neighbourhood of the ends of the overlap enable one to determine the stresses in areas between the angular singularities of the butts and the bulk section in uniaxial traction and so, eventually, to improve the boundary conditions used in analytical computations.

2.2. Test of Specimens

During a traction test of a joint, strains measured with gauges are linear with load at the beginning, but if a microcrack occurs in the adhesive, the microstrain profile measured along the outer surface of the adherend in front of the microcrack is perturbed. So, at each strain gauge, a change in the slope of the curve of applied load *versus* microstrain is related to the start of a microcrack or a state change. The beginning of this cracking can be confirmed by the beginning of an acoustic emission[14]. Moreover, the decrease of strain under increasing load (change in the sign of $dF/d\varepsilon$) is the indication of crack extension along the lap under the gauge.

So, for each gauge, the plot of the load, F, *versus* the surface microstrain on the adherends (Figure 2) enables one to know the two following thresholds:

—*FDj*: microcrack beginning threshold under gauge *j* (limit of linear behavior of the gauge *j*). Beyond this limit, microcracks extend in a steady manner;
—*FGj*: flaw propagation threshold under gauge *j* (change of sign of the slope for the curve of load *vs.* microstrain for the gauge *j*). Beyond this limit, microcracks join together and the cracks thus created extend along the overlap in an unsteady manner.

For all the gauges on the same specimen, the *FDj* minimal value determines the limit, FD, of the "global elastic range" of the joint for a traction test.

3. ANALYTICAL COMPUTATION

The first analysis by Volkersen[2,16], or the improved one made by Goland and Reissner[1], give results which show that peel stresses and shear stresses are maximum at the end of the overlap. However, boundary conditions in the adhesive show that

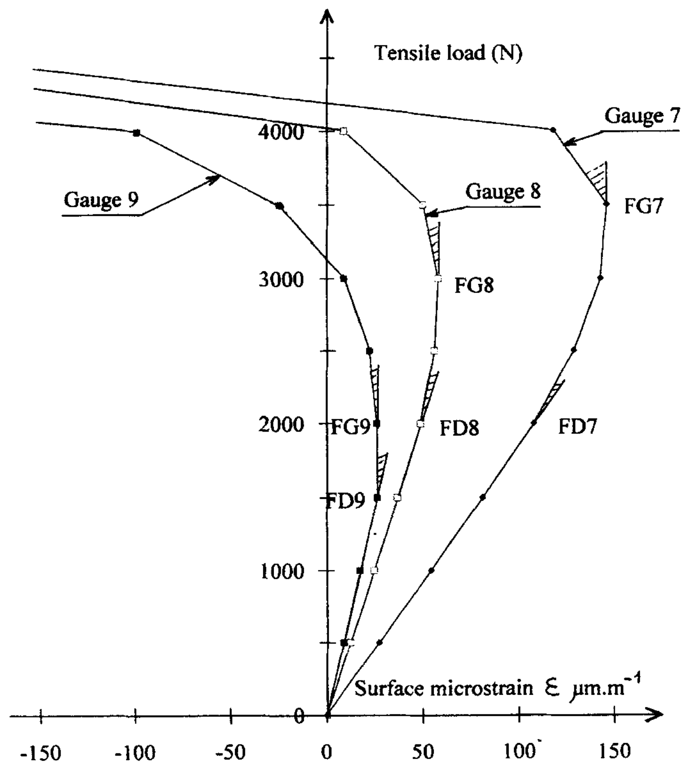

FIGURE 2 Single-lap specimen $X = 23.4$ mm (XC 18/EPONAL 317): plot of the curves of tensile load, F, *versus* "surface microstrain on adherends for the gauges No 7–8 and 9 (in the lap area), in order to detect the thresholds *FDj* and *FGj*.

the shear stresses must become zero at the ends of the lap. Also, if these analyses give pertinent results in the central part of the lap, they are no longer valid at each end of the lap. In fact, knowledge of the stresses near the ends is fundamental because they are the highest here and, experimentally, the early damage of adhesive begins in these places.

An improved calculation method, such as the matched asymptotic expansions method[6], enables to agree with the boundary conditions. In the case of the half-thickness single-lap joint, analytical studies made with the asymptotic expansions method[19] give computed stresses in the adhesive where the shear stress equals zero at the ends, and also enable one to compute strains at the outer surfaces of adherends to compare with experimental results provided by electrical strain gauges.

For the tenon and mortise joint, still with the aid of the asymptotic expansions method, stresses in the adhesive and strains in the adherends have been calculated, with or without a front adhesive layer at each end of the lap[13].

With the formulae extracted from these analytical studies[19], we have computed, for different lengths of the lap and an elastic behaviour, shear stresses and peel stresses (Figures 3 & 4) in the adhesive along the lap, for single-lap joints. The calculations are made for specimens, as shown Figure 1, with adherends made of mild steel ($E = 207700$ MPa and $\nu = 0.29$) and bonded with EPONAL 317 ($E = 5700$ MPa and $\nu = 0.33$), loaded with uniaxial load of 100 Newtons. Shear stress is maximum in the neighbourhood of each extremity of the lap, but is zero at the extremity, where the peel stress is maximum. It is interesting to observe that the maximum of these computed stresses does not vary a lot with the length of the lap. As a matter of fact, the average shear stress decreases as the length of the lap increase, but the shear stresses are concentrated at the ends of the lap.

Figure 5 shows the microstrains at the outer surfaces of the adherends, computed under the same conditions, for several lengths of the lap for single-lap joints. In the

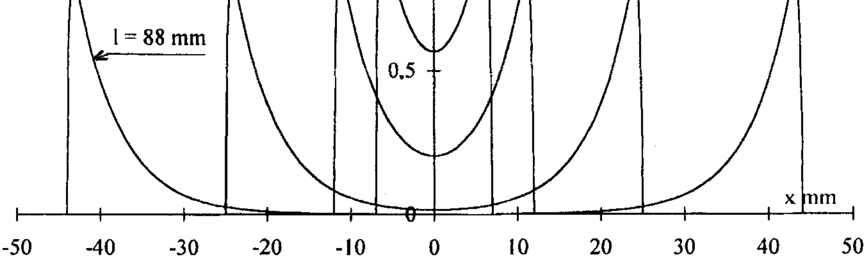

FIGURE 3 Single-lap joints (XC 18/EPONAL 317): computed shear stresses in adhesive along the overlap for different lengths of the lap.

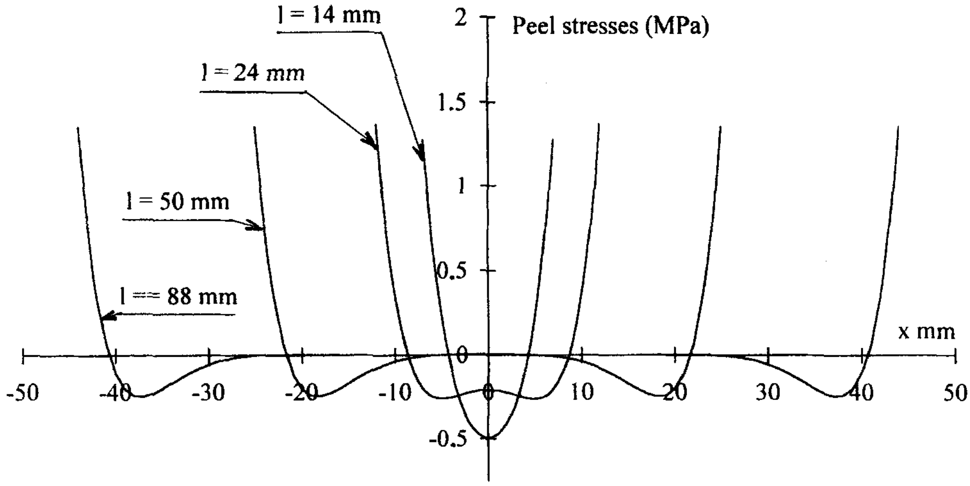

FIGURE 4 Single-lap joints (XC 18/EPONAL 317): computed peel stresses in adhesive along the overlap for different lengths of the lap.

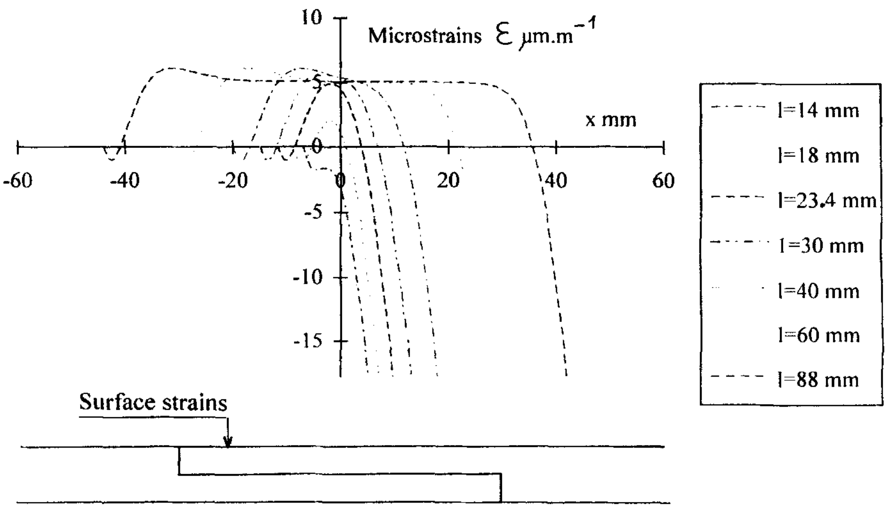

FIGURE 5 Single-lap joints (XC 18/EPONAL 317): computed values of the longitudinal microstrains at the outer surface of adherends along the overlap for different lengths of the lap.

central part, the outer surface is in a traction state. Near the free end, the surface is in small contraction due to a compression or a small flexure of this end. On the other end, near the bulk section of the bar, the contraction is more severe, due to a important flexure given by asymmetry.

4. COMPARISON BETWEEN EXPERIMENTAL AND THEORETICAL ANALYSIS

For single-lap joints, we have studied four lengths of lap. Table I shows the principal mechanical characteristics found in a traction test of these specimens.

Firstly, these experimental results show the high influence of the length of the lap on the value of threshold FD and ultimate tensile strength. These results could not be deducted from examination of the theoretical analysis alone. Besides, they confirm that the ultimate load found in a simple rupture test is unable to give good information on the load for which the damage of the joint begins.

So, with short length of the lap, the global elastic range is difficult to determine with accuracy, but it is very low. For low loads, the mechanical behaviour at each end of the overlap is no longer linear, and this behaviour spreads rapidly over the whole length of the lap. With bigger lengths, the linear behaviour observed at each end is more developed and, when the load increases, nonlinear behaviour does not spread so quickly over the whole length of the lap.

For the four specimens ($l = 14$ mm to 88 mm), we have compared the microstrains measured at the outer surface of the adherends and the values computed from analysis for increasing loads (Figures 6 to 9). In these figures, the theoretical curve with dashes is computed from Berdah's analysis[20], the two others curves from Bensaid's analysis[19], the first (dash + two dots) for simplified theory and the second (dash + dot) for the matched asymptotic expansions method. An early comparison between experimental and theoretical values has been carried out by Berdah[20], but only in the elastic domain, for specimens $l = 23.4$ mm and $l = 37$ mm.

With the shortest length, $l = 14$ mm, even for loads not higher than the upper limit of the global elastic range, agreement is poor at the ends of the lap and satisfactory only over a short distance in the central part. With longer lengths ($l = 23.4$ mm and higher), and a load at the upper limit of the global elastic range, although this load is largely higher than for the shortest length, the agreement is good over the whole length of the lap. Moreover, as shown for the greatest length, $l = 288$ mm, in Figure 9, this agreement still remains acceptable over a large central part of the lap for loads beyond the global elastic range. Of course, the length where

TABLE I
Single-lap specimens: materials used and main mechanical characteristics in a tensile test

Materials adherends/adhesive	length of the lap	ultimate load Newtons	Fd Newtons
FORTAL HR/EPONAL 317	$l = 14$ mm	3000	200
XC 18/EPONAL 317	$l = 23.4$ mm	4500	1500
FORTAL HR/M 3-15	$l = 37$ mm	6000	2000
XC 18/ EPONAL 317	$l = 88$ mm	8000	2000

FORTAL HR: aluminium alloy... E = 72000 MPa $\nu = 0.31$
XC 18: mild steel............ E = 207700 MPa $\nu = 0.29$
EPONAL 317: epoxy resin.........E = 5700 MPa $\nu = 0.33$
M 3-15: epoxy resin..............E = 3360 MPa $\nu = 0.39$

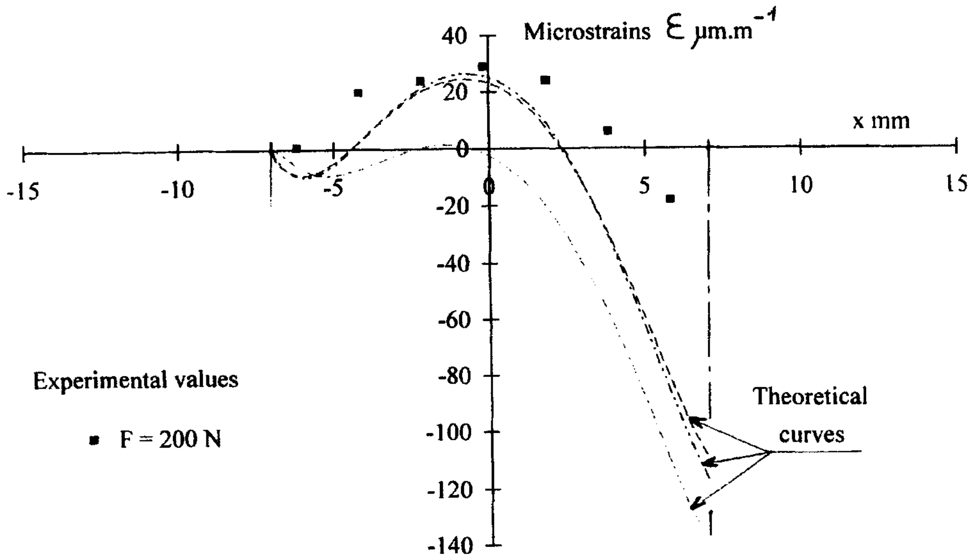

FIGURE 6 Single-lap specimen $l = 14$ mm (FORTAL HR/EPONAL 317): comparison between longitudinal microstrains measured at the outer surface of adherends and theoretical values.

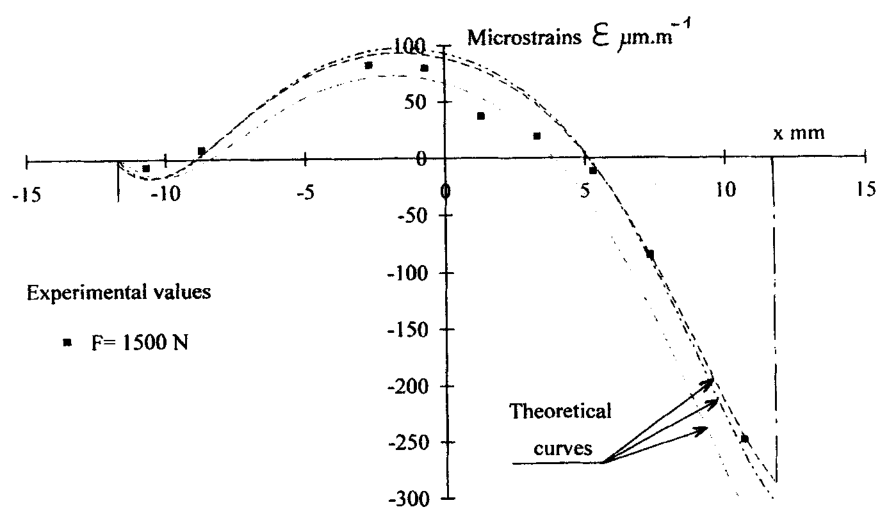

FIGURE 7 Single-lap specimen $l = 23.4$ mm (XC 18/EPONAL 317): comparison between longitudinal microstrains measured at the outer surface of adherends and theoretical values.

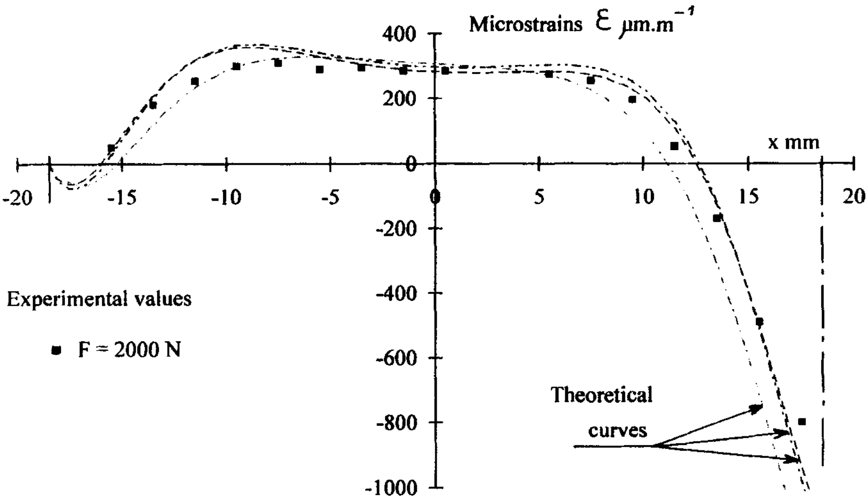

FIGURE 8 Single-lap specimen $l = 37$ mm (FORTAL HR/ M3–15): comparison between longitudinal microstrains measured at the outer surface of adherends and theoretical values.

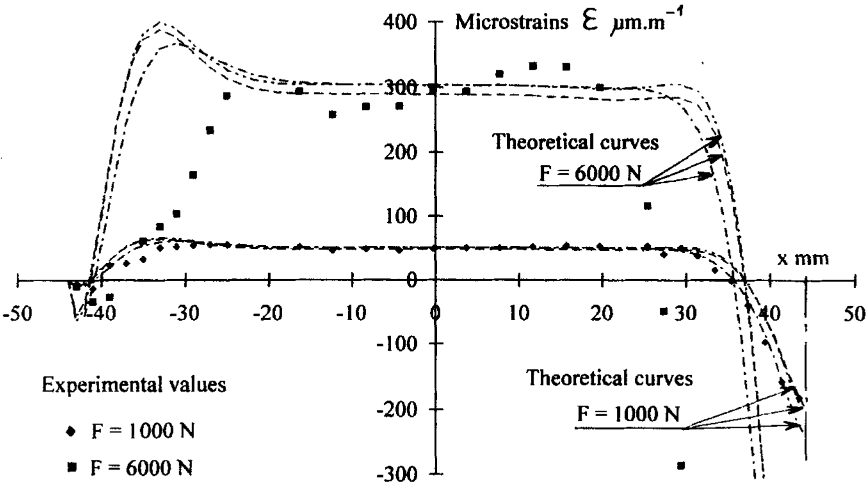

FIGURE 9 Single-lap specimen $l = 88$ mm (XC 18/EPONAL 317): comparison between longitudinal microstrains measured at the outer surface of adherends and theoretical values for two applied loads-1000 N in the global elastic range and 6000 N out of this range.

this agreement is true decreases when the load increases and becomes closer to the ultimate value

In the case of the tenon and mortise joint (Fig. 10), there is no flexure of the adherends of the mortise near the bulk bar and the strain, and so the stress, are the greatest at the bottom of the mortise. Beyond this point, experimentally, we can see that the strain decreases gradually to an average value in the bulk section of the bar.

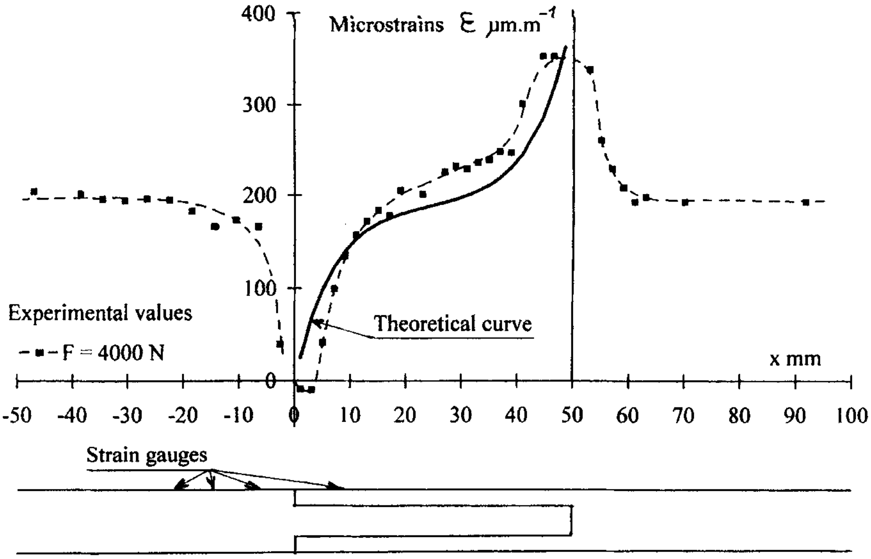

FIGURE 10 Tenon and mortise specimen $l = 50$ mm (XC 18/EPONAL 317): comparison between longitudinal microstrains measured at the outer surface of adherends and theoretical values.

We find the same average value on the other side of the lap in the bar which bears the tenon, as the uniaxial tension is the same at the two ends of the specimen.

In this joint, the global elastic range is narrow ($FD = 500$ N) and the first damage begins near the free end of the mortise around $x = 3$ mm[14]. However, the damage spreads slowly in the adhesive, until the ultimate load ($F = 14500$ N). For $F = 4000$ N, the agreement between experimental and theoretical strains is still acceptable. Nevertheless, the experimental test shows that a small flexure, as in the single-lap joint, takes place at the free end of the mortise but this does not appear in the theoretically computed curve.

5. CONCLUSION

In bonded single-lap joints, theoretical analysis and tests show that maximal stresses and crack initiation occur at or near the ends of the overlap. So, in these areas, the stress concentration is very high, and the elastic limit is exceeded with microcracks starting as soon as the load increases a small amount. Also, the matched asymptotic expansions method, which enables agreement with the boundary conditions, is for short lengths of the lap, not adapted to describe the precise mechanical behaviour in the neighbourhood of the overlap ends, outside of a very narrow range of applied load. In fact, in this case, there is interaction between the two singularities, which are close to each other. Besides, the asymmetry of this joint leads to important flexure of the adherends near the butts. So, the elastic area disappears almost completely.

For a longer length of the lap, firstly, local adaptation of the adhesive, that is similar to plasticity, can occur in the more highly stressed locations. Secondly, damage such as microcracks is confined to the ends for lower loads, and does not spread so quickly along the lap for higher loads. Also, computations are in concordance with experimental results on the major part of the lap, even for a high pulling load.

For the tenon and mortise joint, we have studied here only one length of lap, for which agreement between experimental and analytical results is good. Others tests are presently being carried out with lower and higher lengths of lap to determine the limits of agreement in these cases.

References

1. M. Goland, E. Reissner, "The stress in cemented joints", *J Applied Mechanics*, **11**, A17–A27 (1944).
2. O. Volkersen, "Recherche sur la théorie des assemblages collés", *Construction métallique*, **4**, 3–12 (1965)
3. R. D. Adams, N. A. Peppiat, "Effect of Poisson's ratio strains in adherends on stresses of an idealized lap joint", *J. Strain Analysis*, **8**, No.2, 134 (1973).
4. L. J. Hart-Smith, "Analysis and design of advanced bonded joints", *NASA CR2218* (1974).
5. Y. Gilibert, "Contribution à l' étude de l' adhésivité de matériaux collés par l' intermédiaire de résines époxydiques"; Thèse de Doctorat ès Sciences Physiques, Université de Reims, (1978).
6. Y. Gilibert, A. Rigolot, "Determination of stress distribution in double lap, matched asymptotic expansions and conformal mapping", in *Adhesively Bonded Joints: Testing, Analysis, and Design, ASTMSTP 981*, W. S. Johnson, Ed. (ASTM, Philadelphia, 1988), pp.145–159.
7. Y. Gilibert, A. Rigolot, "Théorie élastique de l' assemblage collé", *RILEM. Matériaux et Constructions*, Dunod Editeur, No.107, pp. 363–387, Sept–Oct. (1985)
8. Y. Gilibert, M. L. L. Klein, "Microcrack initation in adhesive bonded double-lap joints with scarfed ends of outer adherends", *J. Adhesion*, **28**, 51–69 (1989).
9. Y. Gilibert, "Analyse expérimentale du comportement mécanique fin des joints collés époxydiques d' assemblages à double recouvrement biseautés;;, *11th Canadian Congress of Applied Mechanics, Cancam'87*, The University of Alberta, Edmonton, Canada, May 31–June 4 (1987).
10. Y. Gilibert, "Etude expérimentale par extensométrie et émission acoustique simultanées du comportement mécanique fin du joint collé en sifflet à double enture", *XVIIè Congrès de l' AFTPV, Nice*, 1989, C. R. Ed. EREC, Paris (1989).
11. Y. Gilibert, G. Verchery, "Influence of Surface Roughness on Mechanical Properties of Joints", in *ADHESIVE JOINTS, Formation, Characteristics and Testing*, K. L. Mittal Ed. Plenum Press, New York and London, 1984, pp.69–84.
12. Y. Konaté, Y. Gilibert, "Scientific and experimental methodology for elastic moduli determination in a very fragile adhesive joint", *Double Liaison; Physique et chimie des peintures et adhésifs*, Tome XL, N° 454, pp.12–15, (1993).
13. Y. Gilibert, A. Rigolot and R. Tchienkoua, "Theoretical and experimental analysis of the stress-distribution in an adhesive tenon-and-mortise joint" *Proc. EUROPEAN MECHANICS COLLOQUIUM 227, "Mechanical Behaviour of Adhesive Joints"*, Saint-Etienne (France), 31 Aug.–2 Sept 1987, Ed. Pluralis, Paris, pp.151–162, (1987).
14. B. Fargette, Y. Gilibert, L. Rimlinger, "Comportement micro-mascroscopique d' un assemblage collé de type tenon et mortaise sollicité en traction uniaxiale", *Mécanique Industrielle et Matériaux*, GAMI, pp.16–20, Mars (1993).
15. French Patent, Y. Gilibert, No.88 15911, Dec. 25, (1988).
16. O. Volkersen, "Die Nietkraftverteilung in zugbeanspruchten Neitverbeindungen mit konstanten Lascherquerschmitten", *Luftfahrforschung* **15**, 41–47 (1938).
17. Frigyes Thamm, "Stress distribution in lap joints with partially thinned adherends", *J. Adhesion*, **7**, 301–309 (1976).
18. J. B. Sainsbury Carter, "Automated design of bonded joints", *Trans. ASME. J. Engineering for Industry*, Nov 1973, pp. 919–924.
19. A. Bensaid, Y. Gilibert, M. L. L. Klein, "Etudes expérimentale, théorique et numérique par éléments finis, sur micro-ordinateurs, du comportement mécanique fin de l' assemblage collé du type escalier simple", *EUROCOAT 89, XVIIè Congrès A.F.T.P.V.*, Nice (France), C. R. Adhésifs, pp.34–40, Ed. EREC, Paris (1989).

20. C. Berdah, Y. Gilibert, A. Rigolot, "Stress analysis in a single-lap joint subjected to an axial traction force", *ADHESION 87-IIIrd Int. Conf. of Plastics & Rubber Institute*, University of York, England, 7–9 Sept 1987, pp. R1-R6.
21. C. Berdah, Y. Gilibert, A. Rigolot, "Single-lap adhesive bonded joint with axial and transverse symmetries: a theoretical and experimental analysis", *EUROPEAN MECHANICS COLLOQUIUM 227 "Mechanical Behaviour of Adhesive Joints"*, Saint-Etienne (France), 31 Aug.–2 Sept 1987-in proceedings, chapter "Mechanical characterization", pp.199–206, Ed. PLURALIS, Paris (1987).
22. United States Patent, Y. Gilibert, No. 4, 951, 497, Aug. 28, (1990).
23. French Patent, Y. Gilibert, No. 87.155575, Nov. 10, (1987).